JACS
JOURNAL OF THE AMERICAN CHEMICAL SOCIETY

Communication

pubs.acs.org/JACS

Near-Infrared Electrogenerated Chemiluminescence from Aqueous Soluble Lipoic Acid Au Nanoclusters

Tanyu Wang, Dengchao Wang,[†] Jonathan W. Padelford, Jie Jiang,[‡] and Gangli Wang*

Department of Chemistry, Georgia State University, Atlanta, Georgia 30302, United States

Supporting Information

ABSTRACT: Strong electrogenerated chemiluminescence (ECL) is detected from dithiolate Au nanoclusters (AuNCs) in aqueous solution under ambient conditions. A novel mechanism to drastically enhance the ECL is established by covalent attachment of coreactants *N*,*N*-diethylethylenediamine (DEDA) onto lipoic acid stabilized Au (Au-LA) clusters with matching redox activities. The materials design reduces the complication of mass transport between the reactants during the lifetime of radical intermediates involved in conventional ECL generation pathway. The intracluster reactions are highly advantageous for applications by eliminating additional and high excess coreactants otherwise needed. The enhanced ECL efficiency also benefits uniquely from the multiple energy states per Au cluster and multiple DEDA ligands in the monolayer. Potential step and sweeping experiments reveal an onset potential of 0.78 V for oxidative-reduction ECL generation. Multifolds higher efficiency is found for the Au clusters alone in reference to the standard Rubpy with high excess TPrA. The ECL in near-IR region (beyond 700 nm) is highly advantageous with drastically reduced interference signals over visible ones. The features of ECL intensity responsive to electrode potential and solution pH under ambient conditions make Au-LA-DEDA clusters promising ECL reagents for broad applications. The strategy to attach coreactants on Au clusters is generalizable for other nanomaterials.

Electrogenerated chemiluminescence, or electrochemiluminescence (ECL), is initiated by electron-transfer (ET) reactions stimulated by a working electrode at appropriate potentials. Photoemission, ECL, results from chemical and ET processes of those highly reactive radical intermediates following electrode ET reactions.[1] Elimination of the excitation by, i.e., a laser in photoluminescence (PL), greatly simplifies the optics in instrumentation. ECL, as a subcategory of chemiluminescence, has found many applications such as immunoassays and sensing.[2−5] However, there are two major aspects limiting ECL efficiency for better applications. The first is the relative low efficiency due to the intrinsic complex signal generation mechanism involving mass transport and ET dynamics of multiple radical intermediates formed within the proximity of electrode surface.[6,7] The second is environmental factors and competing side reactions that could quench those highly reactive radical intermediates and thus deactivate ECL.[8]

The results here demonstrate two viable routes for better ECL applications particularly for cell and tissue imaging and sensing. The first is to develop aqueous soluble ECL reagents with high efficiency. The challenges include the redox potential window limited by water and reactivity of oxygen, etc.[9−12] Another direction to circumvent the relative low ECL efficiency is to explore ECL in near-infrared (NIR) region by taking advantage of lower background interference and longer penetration depth, etc.[13] Compared to the enhancement achieved in NIR PL, further studies on NIR-ECL, particularly more efficient ECL reagents containing low toxic components, are needed.[2,14] Recent studies on Au nanoclusters (NCs) reveal unique electrochemical and optical properties, particularly the near-IR PL with long lifetime and large Stokes shift, promising energetics for near-IR ECL generation.[15−19]

Au clusters can be described by molecular composition of $Au_xLigand_y$, with various monothiolates being the most widely adopted ligands.[20] Generally, rich electrochemical activities have been reported for organic soluble AuNCs,[21,22] while strong NIR PL from aqueous soluble AuNCs applied for sensing and imaging applications.[23−25] Workentin, Ding et al. pioneered the ECL studies of organic soluble Au clusters founded on those well-established electrochemical properties.[26−30] The ECL is in NIR region consistent with PL and can be significantly enhanced by adopting excess coreactants with matching redox activities. Unfortunately those electrochemical active AuNCs are insoluble in aqueous environment. High excess coreactants and extreme electrode potentials are also needed for the detection of ECL from protein BSA stabilized Au NCs.[31,32] The ECL is primarily in visible region with no discussion of efficiency. NIR-ECL of aqueous soluble AuNCs has not been detected to the best of our knowledge.

In this report, lipoic acid stabilized Au_{22} NCs were synthesized following previous reports.[33−35] The Au-LA NCs were derivatized covalently with *N*,*N*-diethylethylenediamine (DEDA) as shown in Scheme 1 (more details in Scheme S1). New oxidation states on Au-LA NCs due to the multidentate dithiolate binding concept introduced by our group,[36−38] together with tertiary amine as common coreactants, generate oxidative reduction (anodic) ECL.[1] The ECL intensity is in arbitrary unit in all figures (experimental details in SI).

Oxidative reduction ECL is generated through intracluster reduction of the oxidized Au-LA clusters. Representative traces are shown in Figure 1. Both Au-LA NCs and the peripheral DEDAs are oxidized by electrode at similar potentials.

Received: March 23, 2016
Published: May 12, 2016

DOI: 10.1021/jacs.6b03037
J. Am. Chem. Soc. 2016, 138, 6380−6383

Scheme 1. Stepwise ECL Generation of Au-LA-DEDA NCs

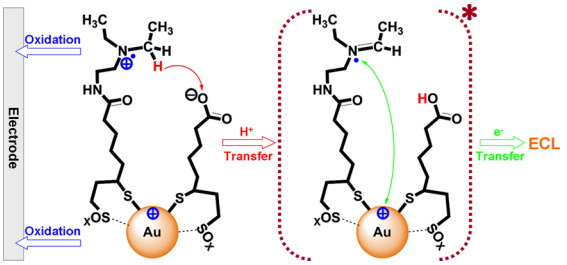

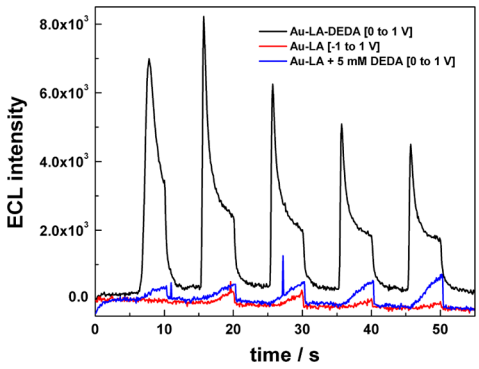

Figure 1. ECL profiles of 6 μM Au-LA NCs with DEDA covalently attached (black), without coreactant (red), and with 5 mM free diffusing DEDA (blue) in solution. The electrode potential was held for 5 s at the denoted potentials and stepped cyclically (5 cycles shown). Data were recorded in 0.1 M $NaClO_4$ under ambient conditions without degassing.

Subsequently, the tertiary amines on the outer ligand monolayer become strong reductant after deprotonation, which reduces the oxidized Au-LA NCs, analogous to the widely adopted Rubpy-TPrA coreactant pathway.[1] Strong ECL can be generated repeatedly by electrode oxidation. As controls, without DEDA in the measurement system, no ECL was detected at comparable electrode potentials (data not shown). However, weak ECL can be generated by a proceeding reduction process prior to electrode oxidation, i.e., the red curve from −1 V to +1 V. This is still impressive being the first self-annihilation ECL detected from aqueous AuNCs to the best of our knowledge. An important notion is that other aqueous soluble monothiolate (i.e., tiopronin and mercaptosuccinic acid) AuNCs do not have ECL under comparable conditions. Following conventional coreactant route, high excess DEDA at 5 mM as coreactants in the solution containing 6 μM Au-LA NCs produced rather weak ECL as well. Unlike most ECL studies, oxygen was not removed during the measurements in an attempt to evaluate ECL performance in broad particularly bioapplicable conditions.

Within each ECL generation cycle, gradual decay in ECL intensity was observed from Au-LA-DEDA, while the two controls increased over time. Without covalent attachment, i.e., conventional ECL pathways, both ECL reagents and coreactants need to be activated separately within the electrode diffuse layer. The ECL generation depends on bimolecular collision/reactions of the two activated radical intermediates governed by their respective lifetime, concentration, and mass transport behaviors. Accordingly, high-excess coreactants are routinely adopted for better efficiency of ECL reagents. The gradual increase is attributed to the accumulation of activated Au cluster intermediates that is better stabilized and protected by the ligand monolayer from environment. In stark contrast to conventional ECL pathways, ECL generation from Au-LA-DEDA NCs is an intracluster process after the electrode activation. The gradual decay results from the relative kinetics of (1) mass transport to the electrode, (2) ET kinetics during electrode oxidation, (3) lifetime of the radical cations, and (4) subsequent charge transfer between the Au cluster and the DEDA molecules in the ligand monolayer. Detailed mechanism and kinetics understanding requires systematic investigation underway.

Correlation of the electrode potential, current, and ECL generation is shown in Figure 2. An ECL onset potential of 0.78

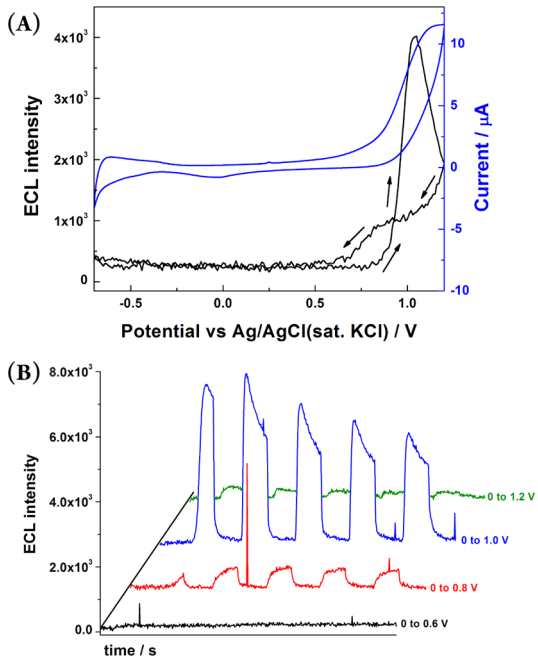

Figure 2. (A) Cyclic voltammogram (top, right axis) and ECL-potential (bottom, left axis) curves for Au-LA-DEDA NCs. For ECL measurement, a Pt mesh was used as working electrode that fits tightly in a thin 1 × 10 cm cuvette for consistency in electrode-camera alignment. The Au-LA-DEDA concentration is ca. ~6 μM. The CV was recorded at a Pt disk electrode (d ~ 0.5 mm) as working electrode. The Au-LA-DEDA concentration is ~1 mM. The supporting electrolyte was 0.1 M $NaClO_4$. Potential scan rate was 0.1 V/s. (B) ECL time traces at different electrolysis potentials. The potential was stepped from a baseline of 0 V to different electrolysis potentials cyclically. Each potential was held for 5 s.

V in the forward scan aligns well with the anodic current peak in the top CV. The oxidation is apparently irreversible from the CV. Accordingly, a hysteresis effect in ECL generation is observed in the backward scan. Irreversible oxidization occurs at comparable potential range for DEDA itself and for the Au-LA NCs without DEDA shown in the CVs in Figure S1. Although no precipitation in solution or deposition on electrode was observed after repeated and prolonger measurements, the possibility of irreversible decomposition of NC-DEDA could not be ruled out at this time.

Continuous ECL generation at constant potentials is shown in Figure 2B. Below the onset potential, i.e. at +0.6 V, no ET reactions and thus no ECL could be observed. The ECL reaches strongest intensity at around +1.0 V, which is consistent with the potential sweeping results shown in Figure 2A. The decrease in ECL intensity at more positive potentials is likely limited by the chemical stability of the oxidized Au-LA-DEDA under the measurement solution conditions, particularly the presence of

DOI: 10.1021/jacs.6b03037
J. Am. Chem. Soc. 2016, 138, 6380−6383

oxygen in slightly basic pH that would facilitate Au oxidation. Interestingly, a gradual intensity increase over time is observed upon stepping up to +0.8 V instead of the decrease to +1.0 V. Apparently the slow electrode oxidation is the rate-limiting step in the ECL generation chain reactions at less positive potentials, while mass or intracluster charge transport limits ECL generation under sufficient fast electrode activation, i.e., +1.0 V, until stability or side reactions interferes at high overpotentials.

ECL from Au-LA-DEDA NCs at different pHs is shown in Figure 3A. The mechanism of tertiary amine as coreactants for

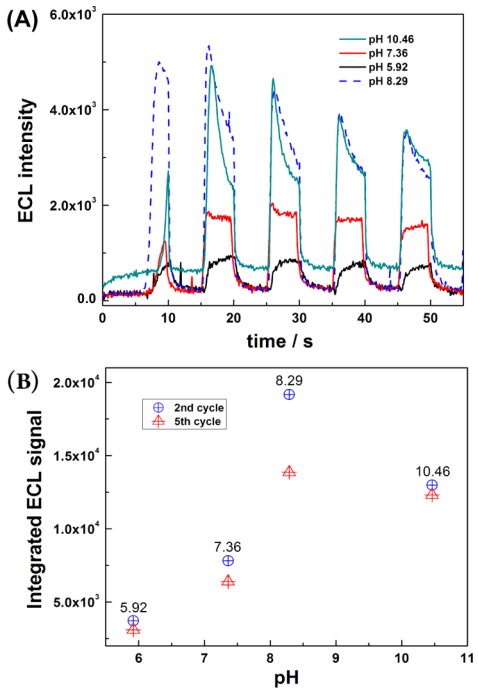

Figure 3. (A) ECL profiles of the Au-LA-DEDA NCs in 0.1 M $NaClO_4$ at different pHs. The electrolysis potential was stepped from 0 to 1 V cyclically. Each potential was held for 5 s. The pH 8.29 curve is the same as the +1.0 V one in Figure 2B for direct comparison. (B) The pH dependence of the integrated ECL signals.

the oxidative reduction ECL generation of Rubpy model system is still under active investigation.[6−8] The general consensus is that deprotonation of the radical cation plays important role. The Au-LA-DEDA solution is slightly basic with a native pH of 8.29, suggesting more tertiary amines than the remaining carboxylic acids in the ligand monolayer. Proton NMR analysis (Figure S2) suggests 7 of the 12 LA were derivatized with DEDA. The two extra tertiary amines (five remaining carboxyl) make the overall cluster slightly basic. The area in each cycle in Figure 3A corresponds to the total or integrated ECL counts. The values from the second and fifth cycle were plotted in Figure 3B to provide a trend over continuous and repeated measurements from the same solution setup. The first cycle is not included due to its much lower intensity that is inconsistent with the later cycles. The possible causes could include stochastic initial conditions at the electrode vicinity at low concentrations (mass transport limited) or, more interestingly and likely, catalytic effects after electrode oxidation that will be systematically address in a follow-up kinetics study. The pH-dependent ECL is exciting for potential sensing of local pH changes, for example, in subcellular organelles or dynamic processes. The pH response range is expected tunable by materials optimization, i.e., ratio of DEDA to remaining COOH during coupling reactions. It is important mentioning that the de/protonation of ligands on clusters is known more gradual spanning over larger pH range compared to the respective weak acid/base. It is therefore anticipated for the AuNC ECL to have a rather broad pH responsive range.

The ECL reaction pathway is proposed to include four key steps (Schemes 1 and 2): (1) electrode oxidation, (2)

Scheme 2. Proposed ECL Mechanism[a]

LA-Au-DEDA → $(^{\cdot}OOC)_{LA}$-Au^{+}-$_{DEDA}(N^{+\cdot}$-$CH_2)$ 1)

P 1) →$(HOOC)_{LA}$-Au^{+}-$_{DEDA}(N^{\cdot}$=CH) 2)

P 2) → LA-Au-$(DEDA\text{-}_{minus}H)^{*}$ 3)

P 3) → LA-Au-$(DEDA\text{-}_{minus}H)$ + *hν* (ECL) 4)

[a]P refers to the product from the corresponding reaction.

deprotonation, (3) annihilation, and (4) ECL emission. The close proximity of the deprotonated COO^{-} from the remaining lipoic acid to the cation radicals from the tertiary amine within the ligand monolayer is highly favorable to stabilize and thus facilitate the formation of cationic radicals by electrostatic interactions and to facilitate deprotonation or the proton transfer as possible acceptors, after which the oxidized Au cluster would be readily reduced by the highly reductive radicals. The electronic coupling between the energy states on the Au core and those molecular orbitals at the core-ligand interface and at the ligand peripheral has been demonstrated which enables charge transfer previously inaccessible for ECL generation and enhancement.[36,37]

At lower pH, the ECL efficiency is reduced due to more protonated COOH and $^{+}HNR_3$ that suppress the deprotonation step. Such pH dependence is consistent with the widely studied Rubyp-TPrA systems.[1] Given there are multiple DEDA per cluster, additional enhancement is expected. Whether the reactions 1−4 (Scheme 2) would be sequential or simultaneous for each DEDA on a cluster will depend on the solution and measurement conditions, which is anticipated to account for, at least partially, the different ECL intensity−time features observed.

The ECL efficiency is estimated by comparing to Rubpy-TPrA system (Figure 4). Both were tested in PBS at pH 8.5 to improve Rubpy ECL. There was no detectable ECL from Rubpy-TPrA at

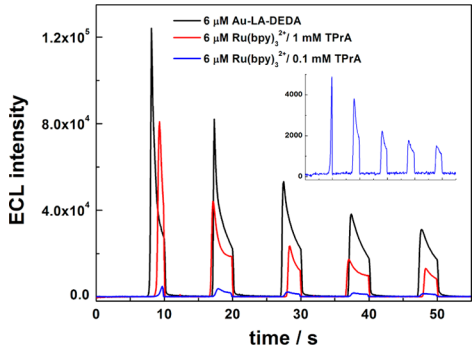

Figure 4. ECL intensity of 6 μM Au-LA-DEDA NCs, 6 μM $Ru(bpy)_3^{2+}$ in the presence of 1 or 0.1 mM of TPrA in 0.2 M PBS, pH 8.5 under ambient conditions without degassing.

DOI: 10.1021/jacs.6b03037
J. Am. Chem. Soc. 2016, 138, 6380−6383

pH below 8.2 under measurement conditions (results not shown).[8] The integrated ECL signal of Au-LA-DEDA is about 1.4 and 17 times higher than that from Rubpy in 1 mM and 0.1 mM TPrA respectively (second cycles). It is worth noting that the Rubpy ECL is rather inconsistent in repeated cycles presumably due to quenching by i.e. oxygen. The intracluster proton and charge transfer not only enhances ECL but also improves ECL stability and makes it more benign to environment factors for better applications.

The emission is primarily in near-IR range consistent with PL. UV−vis absorption and PL spectra of Au-LA NCs before and after DEDA coupling are provided in Figure S3. The emission in near-IR spectrum window is confirmed by adopting different long pass filters (Figure S4); about 83% of total emission intensity remains with a 700 nm long pass filter, while 100% retained with a 650 nm filter.

In summary, intense ECL from AuNCs in aqueous is detected for the first time. Coreactant functionalization and dithiolate bonding provides the required redox states and reactivity otherwise inaccessible. Considering Au-LA-DEDA clusters as nanomolecules, oxidative reduction ECL results from intracluster DEDA-AuLA reactions in a self-annihilation fashion. The emission is demonstrated in NIR region by adopting different filters. The ECL depends strongly on solution pH under ambient conditions without O_2/CO_2 removal. An onset potential of +0.78 V, potential dependence, and continuous ECL generation over seconds is evaluated by potential sweeping and potential step measurements. The ECL from Au-LA-DEDA clusters alone is found multifolds higher than the standard Rubpy system adopting high-excess coreactants TPrA. Broader and more effective applications are envisioned from the reduced background interference in near-IR spectrum region, the elimination of additional coreactants needed in conventional ECL pathways, and the robustness of the ECL under ambient conditions.

■ ASSOCIATED CONTENT

Supporting Information

The Supporting Information is available free of charge on the ACS Publications website at DOI: 10.1021/jacs.6b03037.

Experimental details and data (PDF)

■ AUTHOR INFORMATION

Corresponding Author

*glwang@gsu.edu

Present Addresses

†Department of Chemistry and Biochemistry, Queens College-CUNY, Flushing, New York 11367, United States.

‡PharmaCenter Bonn, Pharmaceutical Institute, Pharmaceutical Chemistry I, University of Bonn, An der Immenburg 4, D-53121 Bonn, Germany.

Notes

The authors declare no competing financial interest.

■ ACKNOWLEDGMENTS

We thank the support of Grant NSF CHE-1059022. J.J. acknowledges the support from the Alexander von Humboldt Foundation

■ REFERENCES

(1) Miao, W. *Chem. Rev.* **2008**, *108*, 2506.
(2) Zhao, W.-W.; Wang, J.; Zhu, Y.-C.; Xu, J.-J.; Chen, H.-Y. *Anal. Chem.* **2015**, *87*, 9520.
(3) Wang, T. Y.; Fan, S. J.; Erdmann, R.; Shannon, C. *Langmuir* **2013**, *29*, 16040.
(4) Miao, W. J.; Bard, A. J. *Anal. Chem.* **2003**, *75*, 5825.
(5) Sentic, M.; Milutinovic, M.; Kanoufi, F.; Manojlovic, D.; Arbault, S.; Sojic, N. *Chem. Sci.* **2014**, *5*, 2568.
(6) Miao, W. J.; Choi, J. P.; Bard, A. J. *J. Am. Chem. Soc.* **2002**, *124*, 14478.
(7) Badocco, D.; Zanon, F.; Pastore, P. *Electrochim. Acta* **2006**, *51*, 6442.
(8) Pastore, P.; Badocco, D.; Zanon, F. *Electrochim. Acta* **2006**, *51*, 5394.
(9) Fang, Y. M.; Song, J.; Li, J. A.; Wang, Y. W.; Yang, H. H.; Sun, J. J.; Chen, G. N. *Chem. Commun.* **2011**, *47*, 2369.
(10) Li, L. L.; Liu, H. Y.; Shen, Y. Y.; Zhang, J. R.; Zhu, J. J. *Anal. Chem.* **2011**, *83*, 661.
(11) Shu, J. N.; Wang, W.; Cui, H. *Chem. Commun.* **2015**, *51*, 11366.
(12) Zou, G. Z.; Liang, G. D.; Zhang, X. L. *Chem. Commun. (Cambridge, U. K.)* **2011**, *47*, 10115.
(13) Ding, Z.; Quinn, B. M.; Haram, S. K.; Pell, L. E.; Korgel, B. A.; Bard, A. J. *Science* **2002**, *296*, 1293.
(14) Wang, J.; Han, H.; Jiang, X.; Huang, L.; Chen, L.; Li, N. *Anal. Chem.* **2012**, *84*, 4893.
(15) Zhang, J.; Fu, Y.; Conroy, C. V.; Tang, Z.; Li, G.; Zhao, R. Y.; Wang, G. *J. Phys. Chem. C* **2012**, *116*, 26561.
(16) Luo, Z. T.; Yuan, X.; Yu, Y.; Zhang, Q. B.; Leong, D. T.; Lee, J. Y.; Xie, J. P. *J. Am. Chem. Soc.* **2012**, *134*, 16662.
(17) Wu, Z.; Jin, R. *Nano Lett.* **2010**, *10*, 2568.
(18) Wang, G.; Guo, R.; Kalyuzhny, G.; Choi, J.-P.; Murray, R. W. *J. Phys. Chem. B* **2006**, *110*, 20282.
(19) Conroy, C. V.; Jiang, J.; Zhang, C.; Ahuja, T.; Tang, Z.; Prickett, C. A.; Yang, J. J.; Wang, G. *Nanoscale* **2014**, *6*, 7416.
(20) Qian, H.; Zhu, M.; Wu, Z.; Jin, R. *Acc. Chem. Res.* **2012**, *45*, 1470.
(21) Laaksonen, T.; Ruiz, V.; Liljeroth, P.; Quinn, B. M. *Chem. Soc. Rev.* **2008**, *37*, 1836.
(22) Murray, R. W. *Chem. Rev.* **2008**, *108*, 2688.
(23) Yu, M.; Zheng, J. *ACS Nano* **2015**, *9*, 6655.
(24) Jiang, Z.; Le, N. D. B.; Gupta, A.; Rotello, V. M. *Chem. Soc. Rev.* **2015**, *44*, 4264.
(25) Treuel, L.; Jiang, X.; Nienhaus, G. U. J. R. *J. R. Soc., Interface* **2013**, *10*, 20120939.
(26) Hesari, M.; Workentin, M. S.; Ding, Z. F. *Chem. Sci.* **2014**, *5*, 3814.
(27) Hesari, M.; Workentin, M. S.; Ding, Z. F. *ACS Nano* **2014**, *8*, 8543.
(28) Lin, C. A. J.; Yang, T. Y.; Lee, C. H.; Huang, S. H.; Sperling, R. A.; Zanella, M.; Li, J. K.; Shen, J. L.; Wang, H. H.; Yeh, H. I.; Parak, W. J.; Chang, W. H. *ACS Nano* **2009**, *3*, 395.
(29) Swanick, K. N.; Hesari, M.; Workentin, M. S.; Ding, Z. F. *J. Am. Chem. Soc.* **2012**, *134*, 15205.
(30) Hesari, M.; Workentin, M. S.; Ding, Z. F. *Chem. - Eur. J.* **2014**, *20*, 15116.
(31) Fang, Y.-M.; Song, J.; Li, J.; Wang, Y.-W.; Yang, H.-H.; Sun, J.-J.; Chen, G.-N. *Chem. Commun.* **2011**, *47*, 2369.
(32) Li, L.; Liu, H.; Shen, Y.; Zhang, J.; Zhu, J.-J. *Anal. Chem.* **2011**, *83*, 661.
(33) Jiang, J.; Conroy, C. V.; Kyetny, M. M.; Lake, G. J.; Padelford, J. W.; Ahuja, T.; Wang, G. J. *J. Phys. Chem. C* **2014**, *118*, 20680.
(34) Shang, L.; Azadfar, N.; Stockmar, F.; Send, W.; Trouillet, V.; Bruns, M.; Gerthsen, D.; Nienhaus, G. U. *Small* **2011**, *7*, 2614.
(35) Aldeek, F.; Muhammed, M. A.; Palui, G.; Zhan, N.; Mattoussi, H. *ACS Nano* **2013**, *7*, 2509.
(36) Wang, D.; Padelford, J. W.; Ahuja, T.; Wang, G. *ACS Nano* **2015**, *9*, 8344.
(37) Ahuja, T.; Wang, D.; Tang, Z.; Robinson, D. A.; Padelford, J. W.; Wang, G. *Phys. Chem. Chem. Phys.* **2015**, *17*, 19342.
(38) Padelford, J. W.; Wang, T.; Wang, G. *ChemElectroChem* **2016** DOI: 10.1002/celc.201600110.

DOI: 10.1021/jacs.6b03037
J. Am. Chem. Soc. 2016, 138, 6380−6383